Domain decomposition for the neutron SP_N equations

E. Jamelot[1], P. Ciarlet, Jr.[2], A.-M. Baudron[1], and J.-J. Lautard[1]

1 Introduction

The neutron transport equation allows to describe the neutron flux density in a reactor core. It depends on 7 variables: 3 for the space, 2 for the motion direction, 1 for the energy (or the speed), and 1 for the time. The energy variable is discretized using the multigroup theory [4]. The P_N transport equations are obtained by developing the neutron flux on the spherical harmonics from order 0 to order N. This approach is very time-consuming. The simplified P_N (SP_N) transport theory [14] was developed to address this issue. The two fundamental hypotheses to obtain the SP_N equations are that locally, the angular flux has a planar symmetry; and that the axis system evolves slowly. The neutron flux and the scattering cross sections are then developed on the Legendre polynomials. The order N is odd, and the number of SP_N odd (resp. even) moments is $\frac{N+1}{2}$.

Let $\mathscr{R}$, the domain of studies, be a bounded, open subset of $\mathbb{R}^3$, with a piecewise smooth boundary. Let $G+1$ be the number of energy groups, and let $g \in \{0,..,G\}$. In the time-independent case, the multigroup SP_N equations read in $\mathscr{R}$:

$$\text{Solve in } (\mathbf{p}^g, \phi^g) \mid \begin{cases} \mathbb{T}_o^g \mathbf{p}^g + \mathbf{grad}\left(\mathbb{H}\phi^g\right) = \sum_{g' \neq g} \mathbb{S}_o^{g'g} \mathbf{p}^{g'}, \\ \mathbb{H}^T \operatorname{div} \mathbf{p}^g + \mathbb{T}_e^g \phi^g = \sum_{g' \neq g} \mathbb{S}_e^{g'g} \phi^{g'} + \frac{1}{\lambda} \chi_g \sum_{g'=0}^{G} \mathbb{M}_f^{g'} \phi^{g'}. \end{cases} \tag{1}$$

For each energy group:

• $\phi^g = (\phi_0^g, \phi_2^g, ...)^T \in \mathbb{R}^{\frac{N+1}{2}}$ (resp. $\mathbf{p}^g = (\mathbf{p}_1^g, \mathbf{p}_3^g, ...)^T \in (\mathbb{R}^3)^{\frac{N+1}{2}}$) denotes the vector containing all the even (resp. odd) moments of the neutron flux.

• $\mathbb{T}_e^g$ (resp. $\mathbb{T}_o^g$) $\in \mathbb{R}^{\frac{N+1}{2} \times \frac{N+1}{2}}$ denotes the even (resp. odd) removal matrix, such that: $\mathbb{T}_e^g = diag\left(\sigma_{r,0}^g, \sigma_{r,2}^g, ...\right)$, $\mathbb{T}_o^g = diag\left(\sigma_{r,1}^g, \sigma_{r,3}^g, ...\right)$, where $\sigma_{r,l}^g$ are proportional to the macroscopic removal cross sections.

• $\mathbb{S}_e^{g'g}$ (resp. $\mathbb{S}_o^{g'g}$) $\in \mathbb{R}^{\frac{N+1}{2} \times \frac{N+1}{2}}$ denotes the even (resp. odd) scattering matrix, such that: $\mathbb{S}_e^{g'g} = diag\left(\sigma_{s,0}^{g' \to g}, \sigma_{s,2}^{g' \to g}, ...\right)$, $\mathbb{S}_o^{g'g} = diag\left(\sigma_{s,1}^{g' \to g}, \sigma_{s,3}^{g' \to g}, ...\right)$, where $\sigma_{s,l}^{g' \to g}$ are proportional to the macroscopic group-transfer cross sections.

• $\mathbb{M}_f^g \in \mathbb{R}^{\frac{N+1}{2} \times \frac{N+1}{2}}$ is such that $(\mathbb{M}_f^g)_{k,l} = \delta_{k,0}\delta_{l,0}\nu_g\sigma_f^g$ (with $\delta_{k,l}$ the Kronecker symbol), so that $\mathbb{M}_f^g \phi^g = (\nu_g \sigma_f^g \phi_0^g, 0, ...)^T$. ν^g is the number of neutrons emitted per fission and σ_f^g the macroscopic fission cross section. χ_g is the fission spectrum.

[1] CEA Saclay, DEN/DANS/DM2S/SERMA/LLPR, F-91191 Gif-sur-Yvette Cedex, e-mail: {Erell.Jamelot}{Anne-Marie.Baudron}{Jean-Jacques.Lautard}@cea.fr .[2] POEMS Laboratory, ENSTA ParisTech, 828, bd des Maréchaux, 91762 Palaiseau Cedex, e-mail: Patrick.Ciarlet@ensta-paristech.fr

- $\mathbb{H} \in \mathbb{R}^{\frac{N+1}{2} \times \frac{N+1}{2}}$ is such that $\mathbb{H}_{k,l} = \delta_{k,l} + \delta_{k,l-1}$.

We must fix boundary conditions (BC) on $\partial\mathscr{R}$, such as Dirichlet BC: $\phi^g = 0$ (zero flux), Neumann BC: $\mathbf{p}^g.\mathbf{n} = 0$ (reflection), or Robin BC (void or isotropic albedo, [2]). From now on, we set zero flux BC.

For simplicity reasons, we will focus on the one-speed SP_N approximation ($G + 1 = 1$). From this study, one can easily deduce the multigroup SP_N case [4], for which we use the Gauss-Seidel method on the energy groups. The group-transfer terms disappear and we can skip the g superscript. We have $\chi_0 = 1$. The linear system (1) corresponds to a set of coupled diffusion equations[1]. Moreover, Eqs (1) can be written in a primal form, with the even moments of the neutron flux as unknowns:

$$-\mathbb{H}^T \text{div}\left(\mathbb{T}_o^{-1}\mathbf{grad}\left(\mathbb{H}\phi\right)\right) + \mathbb{T}_e\,\phi = \frac{1}{\lambda}\mathbb{M}_f\,\phi, \text{ in } \mathscr{R},\, \phi = 0,\text{ on } \partial\mathscr{R}. \qquad (2)$$

Due to the structure of Eqs (2), we remark that Eqs (1) actually correspond to a generalized eigenproblem, where λ acts as the inverse of an eigenvalue with associated eigenflux ϕ. One can apply the Krein-Rutman theorem [9] to Eqs (1): the physical solution is necessarily positive, and it is the eigenfunction associated to the largest eigenvalue $k_{eff} = \max_\lambda \lambda$, which is in addition simple. More precisely, k_{eff} characterizes the physical state of the core reactor:

- if $k_{eff} = 1$: The nuclear chain reaction is self-sustaining. The reactor is critical;
- if $k_{eff} > 1$: The chain reaction races. The reactor is supercritical;
- if $k_{eff} < 1$: The chain reaction vanishes. The reactor is subcritical.

2 The one-domain algorithm

As we look for the smallest eigenvalue $(k_{eff})^{-1}$, it can be computed by the inverse power iteration algorithm. After some initial guess is provided, at iteration $m + 1$, we deduce $(\mathbf{p}^{m+1}, \phi^{m+1}, k_{eff}^{m+1})$ from $(\mathbf{p}^m, \phi^m, k_{eff}^m)$ by solving Eqs (1) with a source term. Set in a domain $\mathscr{R}$, the inverse power iteration algorithm reads:

Set $(\mathbf{p}^0, \phi^0, k_{eff}^0)$, $m = 0$.
Until convergence, do: $m \leftarrow m + 1$

Solve in $(\mathbf{p}^{m+1}, \phi^{m+1})$:

$$\begin{cases} \mathbb{T}_o\,\mathbf{p}^{m+1} + \mathbf{grad}\left(\mathbb{H}\,\phi^{m+1}\right) = 0, \text{ in } \mathscr{R}, \\ \mathbb{H}^T\,\text{div}\,\mathbf{p}^{m+1} + \mathbb{T}_e\,\phi^{m+1} = (k_{eff}^m)^{-1}\mathbb{M}_f\,\phi^m, \text{ in } \mathscr{R}, \\ \phi^{m+1} = 0, \text{ on } \partial\mathscr{R}. \end{cases} \qquad (3)$$

Compute: $k_{eff}^{m+1} = k_{eff}^m \int_\mathscr{R}(\nu\sigma_f\,\phi_0^{m+1})^2 / \int_\mathscr{R}(\nu\sigma_f\,\phi_0^{m+1}\,\nu\sigma_f\,\phi_0^m)$.

End

---

[1] Note that the SP_1 equations are similar to the neutron mixed diffusion equations.

Above, the Eqs (3) with unknowns $(\mathbf{p}^{m+1}, \phi^{m+1})$ model the so-called source solver, with a source term equal to $(k_{eff}^m)^{-1} s_f^m$, where $s_f^m = \nu \sigma_f \phi_0^m$. The updated value k_{eff}^{m+1} is inferred as follows: assuming that convergence is achieved, i.e.

$$\mathbb{H}^T \operatorname{div} \mathbf{p}^{m+1} + \mathbb{T}_e \, \phi^{m+1} = (k_{eff}^{m+1})^{-1} s_f^{m+1}, \tag{4}$$

one can write $(k_{eff}^{m+1})^{-1} s_f^{m+1} = (k_{eff}^m)^{-1} s_f^m$ and, multiplying this equation by s_f^{m+1} and integrating over the domain of computation $\mathscr{R}$, we obtain the equation below (3). The convergence criterion is usually set on $|k_{eff}^{m+1} - k_{eff}^m|$, and $\|s_f^{m+1} - s_f^m\|$. The inverse power iterations are called the outer iterations as opposed to the inner iterations, which correspond to the iterations of the source solver, with a source S. It reads:

$$\text{Solve in } (\mathbf{p}, \phi) : \begin{cases} \mathbb{T}_o \, \mathbf{p} + \mathbf{grad} \left(\mathbb{H} \, \phi \right) = 0, \text{ in } \mathscr{R}, \\ \mathbb{H}^T \operatorname{div} \mathbf{p} + \mathbb{T}_e \, \phi = S, \text{ in } \mathscr{R}, \\ \phi = 0, \text{ on } \partial \mathscr{R}. \end{cases} \tag{5}$$

In the MINOS solver [1, 2], these equations are solved with Raviart-Thomas-Nédélec FE (RTN FE) on a Cartesian or hexagonal mesh. In order to reduce memory size and time computation, we encoded a DD method to solve (5), studied below.

3 Optimized Schwarz method

In order to use non overlapping subdomains, we chose the Schwarz iterative algorithm with Robin interface conditions to exchange information [11]. Let us split $\mathscr{R}$ in two non-overlapping subdomains $\mathscr{R}_1$ and $\mathscr{R}_2$: $\overline{\mathscr{R}} = \overline{\mathscr{R}}_1 \cup \overline{\mathscr{R}}_2$ such that $\mathscr{R}_1 \cap \mathscr{R}_2 = \emptyset$. We define the interface $\overline{\Gamma} = \overline{\mathscr{R}}_1 \cap \overline{\mathscr{R}}_2$. Let $\mathbf{n}_i$ be the outward unit normal vector to $\partial \mathscr{R}_i$, and $(\mathbf{p}_i, \phi_i) = (\mathbf{p}, \phi)_{|\mathscr{R}_i}$. The Schwarz algorithm reads [5]:

Set $(\mathbf{p}_i^0, \phi_i^0)_{i=1,2}$, $n = 0$.
Until convergence, do: $n \leftarrow n + 1$

  Solve in $(\mathbf{p}_i^{n+1}, \phi_i^{n+1})_{i=1,2}$:

$$\begin{cases} \mathbb{T}_o \, \mathbf{p}_i^{n+1} + \mathbf{grad} \left(\mathbb{H} \, \phi_i^{n+1} \right) = \mathbf{Q}, \text{ in } \mathscr{R}_i, i = 1, 2, \\ \mathbb{H}^T \operatorname{div} \mathbf{p}_i^{n+1} + \mathbb{T}_e \, \phi_i^{n+1} = S, \text{ in } \mathscr{R}_i, i = 1, 2, \\ \phi_i^{n+1} = 0, \text{ on } \partial \mathscr{R}_i \cap \partial \mathscr{R}, i = 1, 2, \\ \mathbf{p}_1^{n+1}.\mathbf{n}_1 + \alpha_1 \phi_1^{n+1} = -\mathbf{p}_2^n.\mathbf{n}_2 + \alpha_1 \phi_2^n, \text{ on } \Gamma, \\ \mathbf{p}_2^{n+1}.\mathbf{n}_2 + \alpha_2 \phi_2^{n+1} = -\mathbf{p}_1^{n(+1)}.\mathbf{n}_1 + \alpha_2 \phi_1^{n(+1)}, \text{ on } \Gamma. \end{cases} \tag{6}$$

  End

Here, the Robin parameters are matrices $\alpha_i \in \mathbb{R}^{\frac{N+1}{2} \times \frac{N+1}{2}}$: hence the Robin interface condition can couple all harmonics. The discretization of Eqs (6) with RTN FE is described in [7] for the SP_1 case. Compared to the Schur complement method [10], this method requires less modifications, and rather easy to implement, provided one

has at hand a subdomain solver for the source problem. One has only to ensure the data transfer between the subdomains given by the interface conditions. The $n(+1)$ superscript indicates that we can use either the additive Schwarz method (ASM), or the multiplicative Schwarz method (MSM). We showed in [6, 7] the convergence of the sequences $(\mathbf{p}_i^{n+1}, \phi_i^{n+1})_{i=1,2}$, $n \geq 0$ to $(\mathbf{p}, \phi)_{|\mathscr{R}_{i=1,2}}$ (in the case $\alpha_1 = \alpha_2$). It is well known that the convergence rate depends highly on the Robin matrices $(\alpha_i)_{i=1,2}$. In order to choose them optimally and automatically, we carried out an asymptotic study, à la Nataf and Nier [12]. For the SP_1 case, we obtained that $\alpha_i = (\sigma_{r,0|\mathscr{R}_j})^{1/2}(\sigma_{r,1|\mathscr{R}_j})^{-1/2}$ [7]. We refer to [6] for the computations of the SP_N case, $N > 1$. In this case, the Robin matrices $(\alpha_i)_{i=1,2}$ are symmetric positive definite, and they depend on the removal cross sections values in $(\mathscr{R}_j)_{j=2,1}$. In the multigroup case, the cross sections depend moreover on the energy groups and so do the $(\alpha_i)_{i=1,2}$. Let us see next how this algorithm modifies the eigenvalue algorithm.

4 The multi-domains algorithm

Applying the Schwarz iterative method to algorithm (3), at iteration $m + 1$, we should compute the solution to the source solver iteratively, which yields in principle nested outer ($m \leftarrow m + 1$) and inner (index n) iterations. However, numerical experiments show that the inverse power algorithm leads the global convergence: a single inner iteration is sufficient. So, the resulting algorithm contains only one level of iteration (with index m). The inverse power algorithm with DD reads then:

Set $((\mathbf{p}_i^0, \phi_i^0)_{i=1,2}, k_{eff}^0)$, $m = 0$.
Until convergence, do: $m \leftarrow m + 1$

Solve in $(\mathbf{p}_i^{m+1}, \phi_i^{m+1})_{i=1,2}$, with $j = 2, 1$:

$$
\begin{cases}
\mathbb{T}_o \, \mathbf{p}_i^{m+1} + \mathbf{grad}\left(\mathbb{H}\,\phi_i^{m+1}\right) = 0, \text{ in } \mathscr{R}_i, \\
\mathbb{H}^T \operatorname{div} \mathbf{p}_i^{m+1} + \mathbb{T}_e \, \phi_i^{m+1} = (k_{eff}^m)^{-1}\mathbb{M}_f \, \phi_i^m, \text{ in } \mathscr{R}_i, \\
\mathbf{p}_i^{m+1}.\mathbf{n}_i + \alpha_i \phi_i^{m+1} = -\mathbf{p}_j^{m(+1)}.\mathbf{n}_j + \alpha_i \phi_j^{m(+1)}, \text{ on } \Gamma, \\
\phi_i^{m+1} = 0, \text{ on } \partial\mathscr{R}_i \cap \partial\mathscr{R}.
\end{cases}
\tag{7}
$$

Compute: $k_{eff}^{m+1} = k_{eff}^m \sum_{i=1}^2 \int_{\mathscr{R}_i} (\nu\sigma_f \, \phi_{i,0}^{m+1})^2 \, / \, \sum_{i=1}^2 \int_{\mathscr{R}_i} (\nu\sigma_f \, \phi_{i,0}^{m+1} \, \nu\sigma_f \, \phi_{i,0}^m)$.

End

At iteration $m + 1$, convergence is measured on the source, expressed as a vector $\underline{\mathbf{s}}_f$: $\varepsilon_f^{m+1} = \max_{dof} |(\underline{\mathbf{s}}_f^{m+1} - \underline{\mathbf{s}}_f^m)_{dof}| / (\frac{1}{N} \sum_{dof} |(\underline{\mathbf{s}}_f^{m+1})_{dof}|)$. Iterations stop when $\varepsilon_f^{m+1} \leq \varepsilon_f$, where ε_f is given by the user. Let us test our method.

5 Results

To perform computations, we use the MINOS solver [1, 2] of the APOLLO3®[2] neutronics code. The cross sections come from experimental measurements. They take constant values per unit mesh which can be very different from one mesh to another: we face highly heterogeneous problems. We use the following notations:
- Nc: The number of cores.
- N_{DD}: The 3D cartesian (N_{DD}^x, N_{DD}^y, N_{DD}^z) decomposition.
- N_{out}: The number of outer iterations to achieve convergence.
- $Err.$: The (unsigned) difference between the computed and the converged eigen-values, either sequentially or in parallel, times 10^{-5}.
- CPU: The CPU time spent within the MINOS solver, given in seconds.
- $Eff.$ (Tab. 3 and 2 only): The efficiency (in %): namely, $T_1/(Nc \times T_N)$, where T_1 is the total sequential CPU time with a single domain, and T_N is the parallel CPU time on Nc cores with Nc subdomains.

For Tab. 1 and 3, we used Intel Xeon L5640 processors with an infiniband network. For Tab. 2, computations were carried out on the Titane computer, hosted by the CCRT (the CEA Supercomputing Center). For each test, we report, above the results Tables, a resulting (x,y) normalized power distribution map of the calculation (Fig. 1, 2, 3).

The results presented in Tab. 1 concern a $3D$ model of a pressurized water reactor (PWR) core of capacity 900 MWe. We performed computations on a mono-core, on the diffusion approximation, with two energy groups ($G+1 = 2$) and RTN_0 FE. The mesh is of size $(289 \times 289 \times 60)$, which yields more than 40M unknowns. We set $\varepsilon_f = 10^{-5}$. In order to validate our optimization choice, we ran the MSM (with N subdomains), from 1 up to 17340 subdomains.
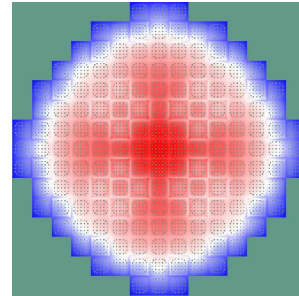

Fig. 1 Power distribution map of the PWR core computation, run with the diffusion approximation, 2 energy groups, RTN_0 FE, MSM.

For $N \leq 4335$, the number of outer iterations does not increase much, and moreover the accuracy is steady. For $N \geq 1156$, the CPU time increase is probably caused by the use of a table to store the subdomains, for which the subdomain access is not

---

[2] APOLLO3 is a trademark registered in France

Table 1 Results of the PWR core computation (diffusion, 2 energy groups, RTN_0, MSM).

N	N_{DD} (x,y,z)	N_{out}	Err. $\times 10^{-5}$	CPU (s)
1	(1, 1, 1)	381	0.0	230
17	(17, 1, 1)	382	0.0	199
289	(17, 17, 1)	393	0.0	210
1 156	(17, 17, 4)	392	0.0	252
2 890	(17, 17, 10)	390	0.0	382
4 335	(17, 17, 15)	394	0.0	499
8 670	(17, 17, 30)	405	0.0	660
17 340	(17, 17, 60)	450	0.1	1 255

optimized yet. On the other hand, the method seems robust: hence, our optimized choice of the Robin parameters is validated in the diffusion case.

We consider now a $3D$ model of a plate-fuel reactor (PFR) core. We performed computations on the SP_5 approximation, with 4 energy groups ($G+1=4$) and RTN_0 FE. The mesh is of size $364 \times 364 \times 100$, which yields 638M unknowns. We set $\varepsilon_f = 5\,10^{-5}$. We ran the ASM on Nc cores with Nc subdomains.
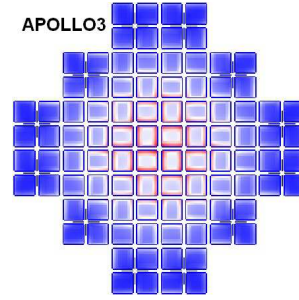
Fig. 2 Power distribution map of the PFR core computation, run with the SP_5 approximation, 4 energy groups, RTN_0 FE, ASM.

Table 2 Results of the PFR core computation (SP_5, 4 energy groups, RTN_0, ASM).

Nc	N_{DD} (x,y,z)	N_{out}	Err. $\times 10^{-5}$	CPU (s)	Eff.
1	(1, 1, 1)	649	0.0	12 272	100%
2	(2, 1, 1)	645	0.0	6 468	95%
4	(2, 2, 1)	644	0.0	3 783	81%
8	(2, 2, 2)	649	0.0	2 269	67%
16	(2, 2, 4)	649	0.0	1 045	73%
32	(4, 4, 2)	654	0.4	504	76%
64	(4, 4, 4)	643	0.3	303	63%
128	(8, 8, 2)	649	0.2	123	155%

Our DD method converges nicely to the sequential solution, since the error on the eigenvalue is always smaller than $5\,10^{-6}$. Moreover, the number of outer iterations

is quite steady: the optimized choice of the Robin parameters is validated in the SP_N case. The method scales quite well, from 67% up to 155% efficiency on 128 cores. To explain this last result, we suppose that the communication traffic was low, second that some computations were performed in the memory cache.

In [6, 7], we give results which show that choosing random Robin matrices leads to worse results: the number of outer iterations increases faster, and the accuracy deteriorates: in practice, it is important to optimize the Robin matrices.

The last results concern a $2D$ model of the Jules Horowitz reactor (JHR) core[3], dedicated to research, which is currently under construction. We performed computations on the SP_1 approximation, with 6 energy groups ($G+1 = 6$), and RT_1 FE. The mesh is of size $10^3 \times 10^3$, which represents more than 72M unknowns. We set $\varepsilon_f = 5\,10^{-4}$.
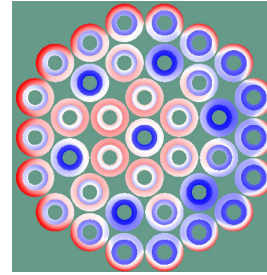

Fig. 3 Power distribution map of the JHR core computation, run with the SP_1 approximation, 6 energy groups, RT_1 FE, ASM.

Table 3 Results of the JHR core computation (SP_1, 6 energy groups, RT_1, ASM).

Nc	N_{DD} (x, y, z)	N_{out}	Err. $\times 10^{-5}$	CPU (s)	Eff.
1	(1, 1)	639	0.0	1487	100%
2	(2, 1)	653	0.4	777	96%
4	(2, 2)	643	0.5	352	106%
8	(2, 4)	653	0.1	256	73%
16	(2, 8)	656	0.2	97	96%
32	(4, 8)	664	0.6	64	73%
64	(8, 8)	653	0.9	29	80%

For this last test, the physical geometry is not Cartesian. It probably explains why the accuracy is not as good as for the other tests. The number of outer iterations is quite steady while the efficiency is excellent. In the case of 4 cores, the superlinear efficiency is probably again a consequence of the amount of computations in the memory cache.

---

[3] http://www.cad.cea.fr/rjh/index.html

6 Conclusions and perspectives

We presented a domain decomposition method based on the optimized Schwarz iterative algorithm, to solve the mixed neutrons SP_N equations with RTN FE. Numerical experiments carried out with the MINOS solver show that the method is robust and efficient both sequentially and in parallel, and that our optimized choice of the parameters of the Schwarz algorithm is satisfactory. Note that the number of iterations to solve our problem increases only slightly with the number of subdomains.

Let us finally mention some potential new research directions:

• The use of Ventcell interface conditions: introducing tangential derivatives in the Robin interface condition [12, 8].

• The use of an overlapping DD method with a coarse grid solver, as done in [13].

Finally, let us mention that the MINOS solver can also solve source and kinetic problems [3].

References

1. Baudron, A.-M., Lautard, J.-J.: MINOS: A Simplified P_N solver for core calculations. Nuclear Science and Engineering **155**, 250–263 (2007)
2. Baudron, A.-M., Lautard, J.-J.: SP_N core calculations in the APOLLO3 System. Mathematics and Computational Methods Applied to Nuclear Science and Engineering (M&C 2011), Latin American Section (LAS) / American Nuclear Society (ANS) (2011)
3. Baudron, A.-M., Lautard, J.-J., Maday, Y., Mula-Hernandez, O.: Parareal for neutronic core calculations. Twenty-first International Conference on Domain Decomposition Methods (2012)
4. Duderstadt, J. J., Hamilton, L. J.: Nuclear reactor analysis. John Wiley & Sons, Inc. (1976)
5. Guérin, P.: Méthodes de décomposition de domaine pour la formulation mixte duale du problème critique de la diffusion des neutrons. Univ. Paris VI (2007)
6. Jamelot, E., Baudron, A.-M., Lautard, J.-J.: Domain decomposition for the SP_N solver MINOS. Transport Theory and Statistical Physics, **41**, 495–512 (2012)
7. Jamelot, E., Ciarlet, P. Jr: Fast non-overlapping Schwarz domain decomposition methods for solving the neutron diffusion equation. J. Comput. Phys. **241**, 445–463 (2013)
8. Japhet, C., Nataf, F., Rogier, F.: The optimized order 2 method: application to convection diffusion problems. Future Generation Computer Systems **18**, 18–30 (2001)
9. Krein, M. G., Rutman, M. A.: Linear operators leaving invariant a cone in a Banach space. Amer. Math. Soc. Translation, Ser. 1, **10**, Functional analysis and measure theory, 199–325 (1962)
10. Lathuilière, B.: Méthodes de décomposition de domaine pour les équations du transport simplifié en neutronique. Univ. Bordeaux I (2010)
11. Lions, P.-L.: On the Schwarz alternating method III: a variant for nonoverlapping subdomains. Third International Symposium Domain Decomposition Methods for Partial Differential Equations (1990)
12. Nataf, F., Nier, F.: Convergence rate of some domain decomposition methods for overlapping and nonoverlapping subdomains. Numer. Math. **75**, 357–377 (1997)
13. Nataf, F. , Xiang, H., Dolean, V.: A two level domain decomposition preconditioner based on local Dirichlet-to-Neumann maps. C. R. Acad. Sci. Paris, Ser. I, **348**, 1163–1167 (2010)
14. Pomraning, G. C.: Asymptotic and variational derivations of the simplified PN Equations. Ann. Nucl. Energy **20**, 9, 623–637 (1993)